Identification of PMN-released mutagenic factors in a co-culture model for colitis-associated cancer

Nicolas Granofszky[#,1], **Michaela Lang**[#,1], **Vineeta Khare**[1], **Gerald Schmid**[1], **Theresa Scharl**[2], **Franziska Ferk**[3], **Kristine Jimenez**[1], **Siegfried Knasmüller**[3], **Christoph Campregher**[*,1], and **Christoph Gasche**[*,1]

[1]Christian Doppler Laboratory for Molecular Cancer Chemoprevention, Division of Gastroenterology and Hepatology, Department of Medicine 3, Medical University of Vienna, Vienna, Austria

[2]ACIB GmbH, c/o Institute of Applied Statistics and Computing, University of Natural Resources and Life Sciences, Vienna, Austria

[3]Institute of Cancer Research, Department of Medicine I, Medical University of Vienna, Vienna, Austria

[#] These authors contributed equally to this work.

Abstract

Microsatellite instability (MSI) is present in ulcerative colitis (UC) and colitis-associated colorectal cancers (CAC). Certain factors released by polymorphonuclear cells (PMNs) may drive mucosal frameshift mutations resulting in MSI and cancer. Here, we applied a co-culture system with PMNs and colon epithelial cells to identify such culprit factors. Subjecting HCT116 + chr3 and human colonic epithelial cells (HCEC)-1CT MSI-reporter cell lines harboring mono-, di- or tetranucleotide DNA repeats linked to enhanced green fluorescent protein (EGFP) to activated PMNs induced frameshift mutations within all repeats, as quantified by flow cytometry. Activated PMNs released superoxide and hydrogen peroxide (H_2O_2), as measured by lucigenin-amplified chemiluminescence and fluorometry, respectively. Catalase, which scavenges H_2O_2, reduced such PMN-induced MSI. The NADPH-oxidase inhibitor apocynin, which blocks the oxidative burst in PMNs, similarly inhibited PMN-induced MSI. A bead-based multiplex assay revealed that PMNs release a wide range of cytokines such as interleukin (IL)-8, IL-6 and tumor necrosis factor-α (TNF-α). *In vitro*, these cytokines increased MSI in colon epithelial cells, and the Janus kinase (JAK) inhibitor tofacitinib abolished IL-6-induced or PMN-induced MSI. Intracellular reactive oxygen species (ROS) formation, as measured by 2',7'–dichlorofluorescein diacetate (DCFDA) assay, was induced upon cytokine treatment. DNA oxidation upon IL-6 was present, as detected by formamidopyrimidine glycosylase (FPG)-modified comet assay. In conclusion, activated PMNs

[*]To whom correspondence should be addressed. Tel: +43 1 40400 47640; Fax: +43 1 40400 47350; christoph.gasche@meduniwien.ac.at; Correspondence may also be addressed to Christoph Campregher, Ph.D. Tel: +43 1 5037244-915; Fax: +43 1 5037244 5; christoph.campregher@aoporphan.com.

induce frameshift mutations in colon epithelial cells resulting in MSI. Both oxidative burst with release of ROS and PMN-secreted cytokines, such as IL-8, IL-6 or TNF-α, contribute to MSI. ROS scavengers and/or specific inhibitors of cytokine signaling may delay or prevent cancer development in the setting of colitis.

Introduction

Ulcerative colitis (UC) is associated with an increased risk for the development of colorectal cancer (CRC). Epithelial cells of the inflamed mucosa accumulate genetic alterations even before any histological evidence of dysplasia or colitis-associated colorectal cancer (CAC) (1–5). Oxidative stress is a recognized driver of mutations in CRC, colitis (6) and CAC (7). UC is considered an 'oxyradical overload' disease in which degranulating polymorphonuclear cells (PMNs) induce certain cellular damage including DNA mutations (8) and thereby contribute to mutagenesis (1,9). It was hypothesized that reactive oxygen species (ROS) or reactive nitrogen species may overwhelm intracellular DNA repair pathways leading to microsatellite instability (MSI) (10), a characteristic of a subset of CRC and other cancers. In fact, MSI, due to deficiencies in the mismatch repair (MMR) system, is detected in 15% of all CRCs; 3% of them is caused by Lynch syndrome (formerly named hereditary non-polyposis CRC), a common familial cancer syndrome (11). MSI-high tumors are associated with immune cell infiltrates. More general, about 20% of all cancers arise in association with chronic inflammation, and most solid tumors contain inflammatory infiltrates where cytokines and chemokines may promote proliferation of tumor cells, perturb their differentiation and support their survival (12,13) and thus create a pro-tumorigenic microenvironment. Also, certain cytokines, such as interleukin (IL)-6, tumor necrosis factor-α (TNF-α), can be produced by PMNs and are increasingly recognized in promoting tumor initiation, progression and metastasis (14–16). Only recently, it has been shown that IL-6 may induce elevated microsatellite alterations at selected tetranucleotide repeats (EMAST), which is also commonly found in inflamed mucosa (17). Although in the setting of infectious colitis the role of PMNs is considered primarily beneficial (9), the PMN infiltration of colonic crypts resulting in crypt abscesses in UC leads to mucosal injury, local inflammation and DNA damage.

Here, we hypothesize that certain secreted products from degranulating PMNs enhance replication errors and frameshift mutations in colonic crypts. In this study, we established a direct co-culture system with activated PMNs and colon epithelial cells to test for the induction of frameshift mutations (18,19). The reporter system involved various pIREShyg2-enhanced green fluorescent protein (EGFP) plasmids each harboring a mono-, di- or tetranucleotide repeat upstream of EGFP and allowed a screen for PMN-secreted products which drive colonic mutagenesis. The identification of such products may help to develop specific compounds for chemoprevention in the setting of UC.

Materials and methods

Cell lines

Various established EGFP-based reporter clones (20,21) were created to compare mutations of mono-,di- and tetranucleotide repeats in human CRC cells [HCT116 + chr3 (22), which has one hmutL homologue 1 (MLH1) wild-type allele transferred through chromosome 3] and primary immortalized human colonic epithelial cells (HCEC)-1CT (23). HCT116 + chr3 single cell clones harboring G16, A10, [CA]13 and [CA]26 repeats were established previously (20,24). Insertion of a single plasmid was verified by Southern blot, and sequence analysis of the EGFP region containing the microsatellites within stable single cell clones was performed upon creation of the cells (20,24). HCEC-1CT stably transfected with EGFP-based plasmids (pIREShyg2-EGFP) harboring A10, [CA]13 and [CA]26 repeats were newly established for this work as performed previously for HCEC-1CT-[AAAG]17 (19). Hygromycin B was used for selection of stable transfectants. Single cell clones of HCEC-1CT cells did not proliferate (19). Thus, stable HCEC-1CT were mixed populations. Upon resuscitation of HCEC-1CT and HCT116 + chr3 clones for this study, cells were characterized morphologically and expression of MMR proteins (MSH2, MSH3 and MLH1) was verified (19,25). HCEC-1CT were analyzed for E-cadherin expression by Western blot, villin and cytokeratin expression by immunofluorescence upon receipt from Jerry W. Shay laboratory in 2009 (23) before plasmid transfection, to verify epithelial origin. In addition, HCEC-1CT reporter cell lines were fluorescently stained for LGR5 to verify stem cell origin. HCT116 + chr3 clones were cultured in IMDM (Gibco/life technologies) containing 4 mM L-glutamine, 10% fetal bovine serum (Biochrom, Berlin, Germany), 150 μg/ml hygromycin B (Gibco) and 400 μg/ml G418 (Gibco). HCEC-1CT were grown in a 4:1 mixture of DMEM (Gibco) and Medium 199 (Gibco) supplemented with 2% calf serum (Hyclone), 50 μg/ml gentamicin (Sigma), 1 μg/ml hydrocortisone (Sigma), 20 ng/ml recombinant human epidermal growth factor (BD Biosciences), 5 nM sodium selenite (Gibco), 2 μg/ml transferrin (Gibco), 10 μg/ml insulin (Gibco) and 300 μg/ml hygromycin B. HCEC-1CT were cultured in 75 cm^2 Primaria cell culture flasks (BD Falcon). Cells were incubated at 37°C, 95% humidity and 5% CO_2. Upon reconstitution, cells were not kept longer than 3 months in culture. For some experiments, HCT116 + chr3-[CA]26, -G16, -A10 or HCEC-1CT-[CA]26 were treated with 0.15 nM phorbol-12-myristate-13-acetate (PMA; Sigma-Aldrich, Germany), 1–50 μM hydrogen peroxide (H_2O_2; Sigma), 25 ng/ml IL-6 (BMS341, eBioscience, Vienna, Austria), 25 ng/ml IL-8 (14-8089-63, eBioscience), 25 ng/ml TNF-α (130-094-022, Miltenyi Biotec, Bergisch Gladbach, Germany), 5 mM 5-aminosalicylic acid (5-ASA; Shire, Dublin, Ireland) and/or 2 μM tofacitinib, a Janus kinase (JAK) inhibitor (CP-690550, Invivogen, San Diego, CA) for 24 h, washed with PBS and measured by flow cytometry after 6 to 8 days.

Isolation and activation of PMNs

PMNs were freshly isolated from blood of healthy donors. Blood was mixed with ½ volume ice-cold dextran solution [2% Dextran T500 (Pharmacia), 0.9% NaCl] followed by sedimentation for 30 min. The upper phase harboring the majority of PMNs was applied on a Ficoll-Paque gradient (GE Healthcare) followed by centrifugation for 20 min at 400g and 15°C. The pellet was resuspended in 15 ml chilled 0.2% NaCl for 45 s to lyse remaining

erythrocytes. Physiological osmolarity was recovered by addition of 15 ml chilled 1.6% NaCl. PMNs were centrifuged for 3 min at 400g and 15°C, washed in Ca/Mg-free Hank's balanced salt solution (HBSS) (Gibco) and counted using a hemocytometer. PMNs were activated with 0.5 nM PMA, if not stated otherwise, in cell culture medium.

Cell sorting, co-culture, flow cytometry, analysis of mutations and calculation of mutation rates

5×10^3–1×10^4 EGFP-negative HCT116 + chr3 or HCEC-1CT frameshift-reporter cells were sorted into 24-well plates on a FACSAria cell sorter using CloneCyt Plus software (BD Biocsiences, San Jose, CA). Twenty-four hours later, freshly isolated PMNs were added together with 0.5 nM PMA at effector:target ratios ranging from 0:1 (control) to 75:1. After 24 h, PMN debris and medium were removed by washing with PBS. Fresh culture medium was added, and target cells were grown for another 6 days. For some experiments PMNs were treated with superoxide dismutase (SOD; Sigma, S7571), apocynin (Santa Cruz, sc-203321) or catalase (Sigma, C3155) at indicated concentrations. After 24 h, medium was renewed.

Target cells were detached using 160 μl accutase (PAA Laboratories GmbH, Linz, Austria) and analyzed on a CellLabs Quanta flow cytometer (Beckman Coulter, Brea, CA). Flow cytometric analysis and calculation of mutation rates (MRs) were performed as described previously (18,20). Data are presented as fold changes to control cells (±95% confidence interval). Also for HCEC-1CT, although mixed clones, fold changes for MRs were calculated, assuming one plasmid insertion in each clone (18).

Analysis of PMN-released superoxide

Release of superoxide (O_2^-) was analyzed using a lucigenin-amplified chemiluminescence assay as described previously (25). Briefly, 7.5×10^4 freshly isolated PMNs were activated with 0.1–5 nM PMA in 500 μl HBSS and 20 μM lucigenin.·O_2^- release was measured between 10 min and 3 h upon activation on a tube luminometer (Lumat LB 9507, Berthold Technologies) and was expressed as relative light units. Single measurements were performed.

Analysis of PMN-released H_2O_2

H_2O_2 was fluorometrically detected using a H_2O_2 Assay (Abcam) according to the manufacturer's protocol. Briefly, 7.5×10^4 or 1.5×10^5 freshly isolated PMNs were activated with 0.5 or 10 nM PMA for 30 min. Fifty microliter of the cell supernatant or H_2O_2 standard dilutions were mixed with 50 μl horse radish peroxidase/OxiRed probe reaction mix. After 10 min, the red-fluorescent dye was measured using a Chameleon V microplate reader (Ex/Em = 485/535 nm; Hidex, Turku, Finland) and absolute amounts of H_2O_2 were calculated. Measurements were carried out in duplicates. For H_2O_2 release upon apocynin treatment, 7.5×10^4 freshly isolated PMNs were activated with 10 nM PMA and treated with 0–200 μM apocynin for 30 min. Measurements were carried out in quadruplicates.

Multiplex immunoassay

A bead-based multiplex assay (Bio-Plex; BioRad, Hercules, CA) was used to detect PMN-released cytokines upon PMA or lipopolysaccharide (LPS)-activation. 2×10^6 PMNs/ml were activated with 0.5 nM PMA or 1 or 10 µg/ml LPS for 16 h. Supernatants were collected and immediately frozen in liquid nitrogen. The bead-based multiplex assay was performed according to the manufacturer's protocol and beads were measured on a Bio-plex 200 instrument (Biorad). A total of 22 cytokines and growth factors (macrophage inflammatory protein-1β, IL-8, vascular endothelial growth factor, intercellular adhesion molecule-1, IL-1 receptor antagonist, IL-17, MCP-1, interferon-γ, IL-6, IP-10, granulocyte-macrophage colony-stimulating factor, TNF-α, IL-1β, IL-1α, IL-12, G-CSF, IL-13, IL-2, IL-7, IL-4, IL-10, IL-5) was analyzed. Measurements were carried out in duplicates.

Analysis of intracellular ROS production

To detect intracellular ROS, the $2',7'$-dichlorofluorescein diacetate (DCFDA), Cellular ROS Detection Assay was used, according to manufacturer's protocol (Abcam). The non-fluorescent, cell-permeable DCFDA diffuses into cells, where it is deacetylated by celluar esterases to $2',7'$-dichlorodihydrofluorescin. In the presence of ROS, the dichlorodihydrofluorescin is oxidized to the highly fluorescent 2',7'-DCF and further detected by fluorescence spectroscopy. 5×10^3 HCEC-1CT cells/96-well were grown for 24 h to 70–80% confluence. Cells were treated with 25 ng/ml TNF-α, IL-6 or IL-8 for 15 min, 30 min, 1 h, 2 h or 3 h. Subsequently, cells were washed twice with PBS, 100 µl of 25 µM DCFDA in HBSS was added and incubated for 30 min. Cells were washed with cold PBS, 100 µl HBSS was added and cells were incubated for 10 min at 37°C. Subsequently, fluorescent cells were measured on a Chameleon V microplate reader (Hidex, Ex/Em = 485/535 nm). Measurements were carried out in triplicates.

Cell metabolic activity and proliferation assays

1×10^3 HCT116-chr3-A10 or -[CA]26 cells/well were seeded into 96-well plates and were grown for 24 h. Cells were treated with 0–1000 U/ml catalase, 0–1000 U/ml SOD or 0–800 µM apocynin in triplicates for 48 h. For the metabolic activity assay, 0.5 mg/ml 3-(4,5-dimethylthiazol-2-yl)-2,5-diphenyltetrazolium bromide (MTT, Sigma, M5655) was added to the medium and cells were incubated at 37°C for 3 h to allow formation of formazan crystals. Cells were subjected to a 1:1 dimethyl sulfoxide:ethanol mixture for 10 min and solubilized crystals were measured at 570 nm within 1 h on a plate reader (Anthos 2010). For measuring cell proliferation, the Cyquant NF cell proliferation assay (Invitrogen) was performed, according to protocol. Briefly, cells were washed with HBSS and incubated with 50 µl of 1× dye binding solution for 1 h at 37°C. Fluorescence intensity, as a measure of cellular DNA content, was determined on a Chameleon V microplate reader (Hidex, Ex/Em = 485/535 nm). Measurements were carried out in duplicates.

Comet assay

The comet assay, a single cell gel electrophoresis assay, with lesion-specific enzyme formamidopyrimidine glycosylase (FPG) for the detection of oxidized DNA bases, was performed. Inorganic salts, bovine serum albumin fraction V, dimethyl sulfoxide, ethidium

bromide, NaOH, Trizma base, 2-[4-(2-hydroxyethyl)piperazine-1-yl]ethanesulphonic acid, Triton X-100, trypan blue, ethylenediaminetetraacetic acid disodium salt dihydrate (Na$_2$EDTA) and FPG were purchased from Sigma-Aldrich (Steinheim, Germany) and Dulbecco's PBS (Ca-Mg-free, pH 7.4) from PAA Laboratories GmbH (Pasching, Austria). Low melting point agarose and normal melting point agarose were obtained from Gibco (Paisley, UK).

HCT116 + chr3 cells were treated with 25 μM H$_2$O$_2$, 50–100 ng/ml IL-6 or 0.5 nM PMA for 24 h and subjected to comet assay analysis (26). 1.5×10^5 HCT116 + chr3 cells were transferred to tubes containing PBS, mixed with 0.5% low melting point agarose and transferred to 1% normal melting point agarose coated slides. Slides were immersed in lysis solution (pH 10, 0.1 M Na$_2$EDTA, 2.5 M NaCl, 10 mM Trizma base, prior to use, 1% Triton X-100 and 10% dimethyl sulfoxide were added freshly) over night at 4ºC. After lysis, the slides were washed twice with enzyme reaction buffer {0.1 M KCl, 40 mM 2-[4-(2-hydroxyethyl)piperazine-1-yl]ethanesulphonic acid, 0.5 mM Na$_2$EDTA, 0.2 mg/ml bovine serum albumin, pH 8} for 8 min. To optimize FPG concentrations, calibration experiments with different FPG dilutions (0, 1:1000, 1:3000, 1:5000, 1:7000) were performed. The nuclei were exposed to either 50 μl of the FPG enzyme solution (1:3000 dilution) for 30 min at 37°C or with the enzyme reaction buffer alone after lysis. Subsequently, DNA was allowed to unwind for 30 min in electrophoresis buffer (0.3 M NaOH and 1 mM Na$_2$EDTA, pH > 13). Electrophoresis was carried out for 30 min (300 mA, 1.0 V/cm corresponding to 25 V) at 4°C. Slides were neutralized (0.4 M Trizma base, pH 7.5) twice for 8 min, rinsed in distilled water and air-dried overnight.

For each experimental condition, three slides were prepared and from each, 50 cells were examined under a fluorescence microscope (Nikon EFD-3, Tokyo, Japan) using 25-fold magnification. The DNA was stained with ethidium bromide (20 μg/ml) and the percentage of DNA in tail was analyzed with a computer-aided system (Comet Assay IV, Perceptive Instruments, UK). Cell viability was determined with trypan blue (0.4%). DNA damage was only analyzed in samples with 80% viability.

Immunocytochemistry

5×10^4 HCEC-1CT A10, CA13 and CA26 reporter cell lines were seeded into IBIDI 8-well 15 μm slides and grown for 24 h. Cells were fixed in 3.7% PFA for 15 min at 4°C, permeabilized with 0.1% Triton-X100 in PBS for 12 min at 4°C and blocked with 3% bovine serum albumin, 0.03% NaN$_3$ in PBS (blocking buffer) for 1 h at room temperature (RT). Cells were incubated with LGR5 primary antibody (1:100, Origene, TA503316) for 2 h at RT and rabbit anti-mouse IgG Alexa Fluor 594 (1:1000, ThermoFisher) secondary antibody for 1 h at RT. Nuclear counterstaining was performed using Hoechst, and cells were embedded in citifluor AF1. HCEC-1CT cells were imaged on a IX81 microscope (Olympus).

Statistics

Total cell numbers, H$_2$O$_2$ and O$_2^-$ release, cell proliferation, metabolic activity and DNA oxidation are presented as mean ± SD and significant differences were calculated using

unpaired samples t-test. Statistical analyses were performed using Graphpad Prism 6.02 (Graphpad Software, San Diego, CA). MRs were calculated as shown previously (20) using the maximum likelihood method and the statistical computing environment R Version 3.2.5. MRs are presented as fold changes compared with control (±95% confidence interval) by calculating fold change = [(MR treatment – mean MR control)/mean MR control]. $P < 0.05$ was considered statistically significant.

Results

Establishment of a 24-well co-culture system

To simulate the interactions of PMNs with crypt epithelial cells in UC, we had previously utilized a co-culture system with PMA-activated PMNs and colon epithelial cells separated by a semi-permeable membrane in 6-well plates (25). Here, we improved this system by using 24-well plates without the use of a semi-permeable membrane, thereby reducing the amount of freshly isolated PMNs about 10-fold. A direct cell-to-cell contact also improved the efficiency of such a system as certain ROS have a very limited half-life, and the reduced distance between PMNs and epithelial cells enhances *in vitro* potency of released ROS.

PMA is known to be a strong activator for degranulation of PMNs but has also several other effects in cells and tissues (27). To establish a non-mutagenic PMA concentration, 5×10^3 EGFP-negative HCT116 + chr3-G16 cells were treated with 0.1–5 nM PMA for 24 h. A dose-dependent decrease in cell proliferation paralleled by an increase in MRs within the G16-repeat at concentrations above 0.5 nM PMA were observed, after 6 days of culture (Figure 1A).

To test whether PMA can also trigger degranulation of PMNs, superoxide production was measured using a lucigenin-amplified chemiluminescence assay (28,29). PMNs were incubated with up to 5 nM PMA and 20 μM lucigenin for up to 3 h. The effect levels at 1 nM PMA (Figure 1B). The superoxide release lasted for at least 3 h with a peak after 30 min. Treatment with 0.5 nM PMA demonstrated robust superoxide release. Thus, in the subsequent co-culture experiments, PMA was used at a non-MSI-inducing concentration of 0.5 nM (Figure 1A).

The effector (PMNs) to target (reporter cell lines) ratio was further optimized using HCT116 + chr3-derived reporter cell lines stably transfected with an EGFP-reporter plasmid carrying G16, A10, [CA]13 or [CA]26 repeats (20). Additionally, primary human colorectal epithelial reporter cell lines (HCEC-1CT (19,23)) were newly established to better understand early events in colitis-associated tumorigenesis. HCEC-1CT-derived reporter cells were stably transfected with EGFP-reporter plasmids carrying A10, [CA]13 and [CA]26 repeats for this set of experiments similarly as described for the [AAAG]17 tetranucleotide reporter cells (19). To verify crypt stem cell origin, HCEC-1CT-derived reporter cells were stained for the stem cell marker LGR5+, which was expressed in the cytoplasm and on the membrane of all reporter cells tested, a finding which was reported previously for spheroid HT29 and HCT116 cells (30) and primary colonic epithelial cells (HCECs) (31) (Supplementary Figure 1, available at *Carcinogenesis* Online).

5×10^3 EGFP-negative cells were sorted into 24-well plates and after 24 h co-culturing with PMA-activated PMNs at effector:target ratios ranging from 25:1 to 75:1 for another 24 h, washed and kept in culture for further 6 days. A dose-dependent decrease in cell count was detected in all clones from both HCT116 + chr3 and HCEC-1CT cells (Figure 2A and B, respectively). HCT116 + chr3-G16, HCT116 + chr3-A10, HCT116 + chr3-[CA]13 and HCT116 + chr3-[CA]26 clones showed a sizable increase in frameshift mutations between 1.6- and 2.2-fold at an effector:target ratio of 75:1 (Figure 2A). HCEC-1CT reporter cells were more sensitive to co-culture-induced stress regarding cell viability and revealed a similar increase in frameshift mutations up to 1.9-fold (CA26) at an effector:target ratio of 50:1 (Figure 2B). For subsequent experiments, A10 and [CA]26 reporter clones were used. To investigate whether there is a time-dependent increase in MRs, HCT116 + chr3 [CA]26 reporter cells were treated with activated PMNs at a ratio of 75:1 for 5, 7 or 9 days. The MR after 7 days increased by 1.5-fold ($P = 0.07$), after 9 days to 1.9-fold ($P = 0.07$) compared with the MR at day 5 (Supplementary Figure 2, available at *Carcinogenesis* Online). Naturally, cell number increased over time.

Induction of MSI by H_2O_2

Activated PMNs are known to release H_2O_2 during degranulation. Indeed, in our system, PMNs released H_2O_2 in a cell number- and PMA-dependent fashion (Figure 3A). 7.5×10^4 PMNs released about 1 nmol/ml (=1 μM) H_2O_2 upon activation with 0.5 nM PMA, which is equal to approximately 8×10^9 H_2O_2 molecules per cell. In contrast, non-activated PMNs did not secrete H_2O_2 above the detection limit of the assay.

In order to verify H_2O_2 as a potent driver of MSI, HCT116 + chr3-A10 cells were treated with H_2O_2 for 24 h, medium was exchanged and the MR was measured after 6 days by flow cytometry. A dose-dependent decrease in cell proliferation and increase in MSI were found upon treatment with 1–50 μM H_2O_2 (Figure 3B). One micromolar H_2O_2 was sufficient to induce frameshift mutations. To investigate whether PMN-released H_2O_2 is involved in induction of mutations within microsatellites, catalase, an antioxidant enzyme catalyzing the decomposition of H_2O_2 to H_2O and O_2, was added to the direct co-culture system (32). PMA-activated PMNs and target cells were co-incubated with 250 U/ml catalase, a concentration not affecting metabolic activity or cell proliferation (Supplementary Figure 3A and D, available at *Carcinogenesis* Online) or MR if added to MSI-reporter cells alone (data not shown). Indeed, 250 U/ml catalase counteracted PMN-induced frameshift mutagenesis in HCT116 + chr3-A10, HCT116 + chr3-[CA]26 (Figure 3C) and HCEC-1CT-A10 (Figure 3D) MSI-reporter cell lines by 24%, 31% and 23%, respectively. Increasing catalase concentration beyond 250 U/ml (up to 1000 U/ml) did not further decrease MR (data not shown), suggesting that besides H_2O_2, other PMN-released factors may also act as mutagenic drivers. Although MSI was reduced, no rescue on cell growth was apparent (Figure 3C and D). In summary, these data indicate that H_2O_2 is released by activated PMNs and may induce MSI in the setting of colonic inflammation.

SOD increases PMN-induced frameshift mutations

SOD catalyzes the dismutation of the highly reactive superoxide anion radical (O_2^-), also released by PMNs (33), into oxygen (O_2) and H_2O_2. PMNs were activated with PMA and

added to HCT16 + chr3-A10 concomitantly with 100–500 U SOD, concentrations not affecting metabolic activity and cell growth, as evaluated by MTT and Cyquant cell proliferation assay, respectively (Supplementary Figure 3B and E, available at *Carcinogenesis* Online). Unexpectedly, SOD fostered PMN-induced MR (Figure 4A). As H_2O_2 is an end product of SOD activity and H_2O_2 has a strong pro-mutagenic ability itself, the increase in frameshift mutations upon SOD might be a consequence of generated H_2O_2.

Inhibition of oxidative burst in PMNs is insufficient for complete prevention of MSI

To investigate whether the blockage of the oxidative burst and the subsequent release of ROS/reactive nitrogen species from PMNs is sufficient to reduce frameshift mutations, the NADPH-oxidase inhibitor apocynin was added to the co-culture system. Apocynin is a natural plant-derived compound, known to block the translocation of the p47phox and p67phox subunit to the cell membrane, thereby inhibiting the assembly of NADPH oxidase (34) and subsequent O_2^- production, which can be finally converted to H_2O_2 by SOD. Indeed, apocynin inhibited H_2O_2 release by PMA-activated PMNs in a dose-dependent fashion (Supplementary Figure 4, available at *Carcinogenesis* Online) and an IC50 of 16 μM (± 48). To test apocynin in our co-culture system, PMNs were pre-incubated for 10–15 min with 75 μM apocynin, activated with 0.5 nM PMA and subsequently added to HCT116 + chr3-A10 or HCT116 + chr3-[CA]26 cells. Apocynin did not affect cell proliferation and metabolic activity (Figure 4B, Supplementary Figure 3C and F, available at *Carcinogenesis* Online) or MR if added to HCT116 + chr3 clones alone (data not shown) but reduced PMN-induced MSI by 47% and 31% in HCT116 + chr3-A10 and HCT116 + chr3-[CA]26 cells, respectively, demonstrating only incomplete inhibition of PMN-induced MSI by blockage of the oxidative burst. Thus, other PMN-released factors, such as cytokines, may add to the induction of MSI in the setting of chronic inflammation.

Identification of cytokines released by activated PMNs

Immune cells secrete a wide range of cytokines. Therefore, we quantitatively analyzed which soluble factors are released by PMNs. 2×10^6 freshly isolated PMNs were activated with 0.5 nM PMA or 1 or 10 μg LPS. Supernatants were analyzed using a multiplex bead-based immunoassay.

Upon stimulation of PMNs with 0.5 nM PMA, the majority of cytokines analyzed were secreted at pico- to nanomolar concentrations (Figure 5A). The highest concentrations were found for macrophage inflammatory protein-1β/CCL4, reaching at 20 ng/ml, the upper detection limit of the assay. IL-8/CXCL8 was expressed at 6 ng/ml, followed by 2.2 ng/ml vascular endothelial growth factor, 1.3 ng/ml intercellular adhesion molecule-1, 0.57 ng/ml IL-1 receptor antagonist, 0.13 ng/ml IL-17, 0.12 ng/ml monocyte chemotactic protein-1 MCP-1/CCL2, 64 pg/ml interferon-γ, 39 pg/ml IL-6, 35 pg/ml IP-10/CXCL-10, 34 pg/ml granulocyte-macrophage colony-stimulating factor and 28 pg/ml TNF-α. LPS stimulation at 1 or 10 μg/ml was similar to 0.5 nM PMA (Supplementary Figure 5, available at *Carcinogenesis* Online). In summary, PMNs release a wide range of cytokines and growth factors in cell culture, with macrophage inflammatory protein-1β, IL-8 and vascular endothelial growth factor being most abundant.

Single cytokines induce MSI in colon epithelial cells

IL-6, IL-8 and TNF-α are cytokines which are highly relevant in inflammatory bowel diseases. IL-6, IL-8 and TNF-α are increasingly expressed at sites of inflammation compared with uninflamed areas of the intestinal tissue. Data from mouse models indicate that IL-6, IL-8 and TNF-α may contribute to CAC (35).To test whether certain cytokines may directly induce mutagenesis in dinucleotide repeats, we treated HCT116 + chr3-A10 and HCEC-1CT-[CA]26 clones with IL-8, IL-6 or TNF-α (Figure 5B and C). All three cytokines decreased cell count, with TNF-α being most effective and HCEC-1CT-[CA]26 being most sensitive. Treatment with IL-6, IL-8 and TNF-α resulted in a 0.6-fold, 0.2-fold and 0.7-fold increase of MSI in HCT116 + chr3-A10, respectively. In HCEC-1CT-[CA]26, TNF-α treatment increased frameshift mutations by 3.4-fold, IL-6 and IL-8 by 0.4- and 0.3-fold, respectively. Similar treatment of HCT116 + chr3-G16 with IL-6 also induced mutations (data not shown). This increase in frameshift mutations was accompanied by ROS production in HCEC-1CT cells upon cytokine treatment (Figure 5D). Beyond frameshift mutations, IL-6 also induced oxidative DNA damage as measured by comet assay (Figure 5E), emphasizing the importance of JAK-STAT signaling in cancer progression.

JAK inhibitor attenuates IL-6-induced MSI

The JAK inhibitor tofacitinib is in clinical development for a series of immune-mediated diseases including UC (36), celiac disease (37) and is FDA approved for rheumatoid arthritis (38). Here, we investigated whether tofacitinib affects IL-6-induced MSI. Indeed, tofacitinib abolished IL-6-induced frameshift mutations in HCT116 + chr3-CA (26) (Figure 6A), indicating that inhibition of the JAK-STAT pathway is sufficient to block frameshift mutagenesis.

5-ASA counteracts the mutagenic effect of IL-6

Mesalamine, or 5-ASA, is a well-established drug for the treatment of mild-to-moderate UC with antineoplastic properties and known to decrease MSI both *in vitro* (21,39) and *in vivo* (40). To evaluate whether 5-ASA specifically reduces MRs induced by IL-6, HCT116 + chr3-[CA]26 were treated with 5 mM 5-ASA. Similar to tofacitinib, also 5-ASA counteracted IL-6-induced MSI (Figure 6B).

Tofacitinib, but not 5-ASA counteracted PMN-induced MSI

To evaluate the effect of 5-ASA, tofacitinib or a combination thereof in our co-culture model, HCT116 + chr3-[CA]26 were treated with 5 mM 5-ASA and/or 2 μM tofacitinib before the addition of PMA-activated PMNs. Tofacitinib reduced microsatellite mutations, whereas 5-ASA failed to do so. (Figure 6C) No synergistic or additive effects for the reduction of microsatellite mutations were found upon combinatorial treatment.

Discussion

MSI, specifically at dinucleotide repeats, is an early event of CAC development and can be detected in chronic inflamed mucosa (1–5). Inhibition of MSI in the setting of UC may help preventing CAC. To simulate the carcinogenic environment in the setting of UC, we co-cultured PMNs (the effector cells) with MSI-reporter colon epithelial cells (the targets).

Here, we demonstrate that PMN-derived ROS from oxidative burst play an important role in the induction of MSI in colorectal cells. In addition, PMN-derived cytokines including IL-8, IL-6 and TNF-α also contribute to frameshift mutations within dinucleotide repeats. Such cytokines induce *de novo* ROS production within colonic epithelial cells, and JAK inhibition reduces mutations. Therefore, both ROS scavenging and inhibition of cytokine signaling may prevent cancer development in UC.

During the oxidative burst of degranulating PMNs, a vast amount of various ROS is released. ROS can induce mutations and genomic instability (41–45). Exposure of mammalian cells to hyperoxia can lead to gross rearrangements of DNA rather than point mutations or small deletions (43). Subjecting plasmid DNA carrying monkey kidney cells to H_2O_2 induces base substitutions and short deletions of 1–3 base pairs (44). PMN exposure to replicating human cells carrying plasmid DNA induced deletions and base substitutions, but no 1–2 base pair deletions (45), pointing to different mutational pathways and repair kinetics induced by PMNs versus H_2O_2-induced lesions (44). In addition, other factors secreted by PMNs might contribute to DNA damage. Previously, we could show that exposure of HCT116$^{MLH1-/-}$ to activated PMNs induces a G_2/M cell cycle arrest, indicative of DNA damage repair (25). In addition, PMNs, separated by a semipermeable membrane from colon epithelial cells, increase frameshift mutations within microsatellites in such. Herein, we provide evidence that direct co-culture of activated PMNs with MLH1-proficient colon epithelial cells induces MSI in mono- and dinucleotide repeats. Mono- and dinucleotide repeats were similarly affected in HCT116 + chr3$^{MSH3-/-}$ and HCEC-1CT, whereas tetranucleotide repeat harboring HCEC-1CTs were most sensitive to PMN-induced stress paralleled by cell death at low effector:target ratios. In fact, EMAST is found in chronic inflamed tissue and correlates with a heterogeneous or decreased MSH3 protein (17,46,47). Ulcerated tumors (46) or tumors with CD8$^+$ T-cell infiltrates (48) may present EMAST. Lynch syndrome tumors and some sporadic MSI-H tumors show a high abundance of tumor infiltrating lymphocytes (49,50). Hence, it is not surprising that PMNs induce mutations not only in mono- and dinucleotide repeats but also affect tetranucleotide repeats as a major driver of genomic instability.

As mentioned above, H_2O_2 is secreted by degranulating PMNs and is capable of inducing genomic instability. In our search for the major culprit factor responsible for MSI in the setting of chronic inflammation, we identified H_2O_2 to induce frame-shift mutations in mononucleotide repeats in a concentration-dependent manner. Blocking H_2O_2 with catalase or limiting H_2O_2 production with apocynin reduced MR significantly. Similarly, single strand breaks resulting from the oxidative burst could be counteracted with catalase (51). In contrast, SOD, catalyzing the dismutation of O_2^- to O_2 and H_2O_2, increased MR, emphasizing the importance of H_2O_2 as an inducer of MSI.

Although catalase was able to reduce MSI in our co-culture system, cell growth was not rescued (Figure 3C). Previously, we could show that combined treatment with catalase and SOD was not able to counteract PMN-induced G_2/M arrest, although such treatment reversed H_2O_2-induced G_2/M arrest (25). Besides·O_2^- and H_2O_2, which are catalyzed by SOD and catalase, respectively, other factors released by activated PMNs such as

chlorinating agents (e.g. HOCl) or reactive nitrogen species may lead to cell cycle arrest (without inducing MSI) and thus inhibit proliferation.

PMNs do not only produce ROS but also secrete a panel of cytokines, chemokines and growth factors, independent of the oxidative burst. Certainly, the inflammatory profile of PMNs at the site of inflammation might differ from *in vitro* activated PMNs, but cytokines such as IL-8 (52), IL-6 (53) and TNF-α (54) were shown to be elevated in active UC and Crohn's disease. Treatment of HCT116 + chr3 (MLH1 proficient, MSH3 deficient) and HCEC-1CT (MMR proficient) cells with these cytokines induced MSI. Shown previously, IL-6 treatment of lung and cancer cells leads to a nucleocytoplasmic shuttling of the MMR protein MSH3 and low-dose, long-term IL-6 treatment causes EMAST (17). In our assay, we demonstrate that a single hit of 25 ng/ml IL-6, IL-8 or TNF-α induced frameshift mutations in mono- and dinucleotide repeats. Internal ROS production upon cytokine treatment increased, as also reported by Tseng-Rogenski *et al.*, supporting the hypothesis that oxidative stress by a single cytokine can induce frameshift mutations (17). To counteract ROS production, we co-treated cells with IL-6 and the potent ROS scavenger 5-ASA (39,55,56), a standard drug for the treatment of UC. 5-ASA reduced IL-6-induced MSI, supporting its antineoplastic activity. This was in agreement with previous studies on 5-ASA and MSI *in vitro* (21,39,57) and *in vivo* (40). Even more effective, the JAK inhibitor tofacitinib, successfully tested in three phase 3 placebo-controlled clinical trials for the treatment of UC (36), abolished IL-6-induced mutations. The JAK-STAT pathway is highly affected in inflammation and CAC, with a specific role for IL-6 (16). IL-6 can alter DNA methylation via SOCS3 promoter hypermethylation induced by DNMT1 and subsequent STAT3 overactivation in CAC patients (58,59). Constitutive STAT3 activation leads to a cytoplasmic translocation of hMSH3, similar to treatment with IL-6 (17). Counteracting IL-6-induced mutations with the JAK inhibitor highlights the importance of the JAK-STAT signaling pathway in DNA damage induction upon oxidative stress. Targeting of IL-6 or TNF-α by monoclonal antibodies might dampen mutagenesis, thereby reducing CAC. Clinical data on the chemopreventive properties of any of the anti-TNF drugs are still lacking. Although 5-ASA did not prevent microsatellite mutations in our co-culture model with activated PMNs in contrast to treatment with IL-6 only, a combined approach of another ROS scavenger and a JAK-STAT inhibitor, such as tofacitinib, may further delay or prevent CRC development in the setting of colitis.

Supplementary Material

Refer to Web version on PubMed Central for supplementary material.

Acknowledgements

Abbreviations

|	
5-ASA	5-aminosalicylic acid
CAC	colitis-associated colorectal cancer
CRC	colorectal cancer
DCFDA	2',7'–dichlorofluorescein diacetate
EGFP	enhanced green fluorescent protein
EMAST	elevated microsatellite alterations at selected tetranucleotide repeats
FPG	formamidopyrimidine glycosylase
HCEC	human colonic epithelial cells
H_2O_2,	hydrogen peroxide
IL	interleukin
JAK	janus kinase
LPS	lipopolysaccharide
MLH1	mutL homologue 1
MMR	mismatch repair
MRs	mutation rates
MSI	microsatellite instability
Na_2EDTA	ethylenediaminetetraacetic acid disodium salt dehydrate
PMA	phorbol-12-myristate-13-acetate
PMNs	polymorphonuclear cells
ROS	reactive oxygen species
SOD	superoxide dismutase
TNF-α	tumor necrosis factor-α
UC	ulcerative colitis

References

1. Ullman TA, et al. Intestinal inflammation and cancer. Gastroenterology. 2011; 140:1807–1816. [PubMed: 21530747]

2. Brentnall TA, et al. Microsatellite instability in nonneoplastic mucosa from patients with chronic ulcerative colitis. Cancer Res. 1996; 56:1237–1240. [PubMed: 8640805]

3. Park WS, et al. Loss of heterozygosity and microsatellite instability in non-neoplastic mucosa from patients with chronic ulcerative colitis. Int J Mol Med. 1998; 2:221–224. [PubMed: 9855692]

4. Leedham SJ, et al. Clonality, founder mutations, and field cancerization in human ulcerative colitis-associated neoplasia. Gastroenterology. 2009; 136:542–50.e6. [PubMed: 19103203]

5. Salk JJ, et al. Clonal expansions in ulcerative colitis identify patients with neoplasia. Proc Natl Acad Sci USA. 2009; 106:20871–20876. [PubMed: 19926851]

6. Simmonds NJ, et al. Chemiluminescence assay of mucosal reactive oxygen metabolites in inflammatory bowel disease. Gastroenterology. 1992; 103:186–196. [PubMed: 1319369]

7. Roessner A, et al. Oxidative stress in ulcerative colitis-associated carcinogenesis. Pathol Res Pract. 2008; 204:511–524. [PubMed: 18571874]

8. Barzilai A, et al. DNA damage responses to oxidative stress. DNA Repair (Amst). 2004; 3:1109–1115. [PubMed: 15279799]

9. Fournier BM, et al. The role of neutrophils during intestinal inflammation. Mucosal Immunol. 2012; 5:354–366. [PubMed: 22491176]

10. Loeb KR, et al. Genetic instability and the mutator phenotype. Studies in ulcerative colitis. Am J Pathol. 1999; 154:1621–1626. [PubMed: 10362784]

11. Boland CR, et al. Microsatellite instability in colorectal cancer. Gastroenterology. 2010; 138:2073–2087.e3. [PubMed: 20420947]

12. Grivennikov SI, et al. Inflammatory cytokines in cancer: tumour necrosis factor and interleukin 6 take the stage. Ann Rheum Dis. 2011; 70:i104–i108. [PubMed: 21339211]

13. Klampfer L. Cytokines, inflammation and colon cancer. Curr Cancer Drug Targets. 2011; 11:451–464. [PubMed: 21247378]

14. Fantini MC, et al. Cytokines: from gut inflammation to colorectal cancer. Curr Drug Targets. 2008; 9:375–380. [PubMed: 18473765]

15. De Simone V, et al. Th17-type cytokines, IL-6 and TNF-α synergistically activate STAT3 and NF-kB to promote colorectal cancer cell growth. Oncogene. 2015; 34:3493–3503. [PubMed: 25174402]

16. Grivennikov S, et al. IL-6 and Stat3 are required for survival of intestinal epithelial cells and development of colitis-associated cancer. Cancer Cell. 2009; 15:103–113. [PubMed: 19185845]

17. Tseng-Rogenski SS, et al. Interleukin 6 alters localization of hMSH3, leading to DNA mismatch repair defects in colorectal cancer cells. Gastroenterology. 2015; 148:579–589. [PubMed: 25461668]

18. Gasche C, et al. Identification of frame-shift intermediate mutant cells. Proc Natl Acad Sci USA. 2003; 100:1914–1919. [PubMed: 12578960]

19. Campregher C, et al. MSH3-deficiency initiates EMAST without oncogenic transformation of human colon epithelial cells. PLoS One. 2012; 7:e50541. [PubMed: 23209772]

20. Campregher C, et al. The nucleotide composition of microsatellites impacts both replication fidelity and mismatch repair in human colorectal cells. Hum Mol Genet. 2010; 19:2648–2657. [PubMed: 20421367]

21. Gasche C, et al. Mesalazine improves replication fidelity in cultured colorectal cells. Cancer Res. 2005; 65:3993–3997. [PubMed: 15899787]

22. Koi M, et al. Human chromosome 3 corrects mismatch repair deficiency and microsatellite instability and reduces N-methyl-N'-nitro-N-nitrosoguanidine tolerance in colon tumor cells with homozygous hMLH1 mutation. Cancer Res. 1994; 54:4308–4312. [PubMed: 8044777]

23. Roig AI, et al. Immortalized epithelial cells derived from human colon biopsies express stem cell markers and differentiate *in vitro*. Gastroenterology. 2010; 138:1012–21.e1. [PubMed: 19962984]

24. Gasche C, et al. Oxidative stress increases frameshift mutations in human colorectal cancer cells. Cancer Res. 2001; 61:7444–7448. [PubMed: 11606378]

25. Campregher C, et al. Activated neutrophils induce an hMSH2-dependent G2/M checkpoint arrest and replication errors at a (CA)13-repeat in colon epithelial cells. Gut. 2008; 57:780–787. [PubMed: 18272544]

26. Tice RR, et al. Single cell gel/comet assay: guidelines for *in vitro* and *in vivo* genetic toxicology testing. Environ Mol Mutagen. 2000; 35:206–221. [PubMed: 10737956]

27. Chang MS, et al. Phorbol 12-myristate 13-acetate upregulates cyclooxygenase-2 expression in human pulmonary epithelial cells via Ras, Raf-1, ERK, and NF-kappaB, but not p38 MAPK, pathways. Cell Signal. 2005; 17:299–310. [PubMed: 15567061]

28. Luciani MG, et al. 5-ASA affects cell cycle progression in colorectal cells by reversibly activating a replication checkpoint. Gastroenterology. 2007; 132:221–235. [PubMed: 17241873]

29. Müller-Peddinghaus R. *In vitro* determination of phagocyte activity by luminol- and lucigenin-amplified chemiluminescence. Int J Immunopharmacol. 1984; 6:455–466. [PubMed: 6094369]

30. Wei B, et al. Coaction of spheroid-derived stem-like cells and endothelial progenitor cells promotes development of colon cancer. PLoS One. 2012; 7:e39069. [PubMed: 22745705]

31. Chen HJ, et al. A recellularized human colon model identifies cancer driver genes. Nat Biotechnol. 2016; 34:845–851. [PubMed: 27398792]

32. Evans CA. On the catalytic decomposition of hydrogen peroxide by the catalase of blood. Biochem J. 1907; 2:133–155. [PubMed: 16742049]

33. DeChatelet LR, et al. Effect of phorbol myristate acetate on the oxidative metabolism of human polymorphonuclear leukocytes. Blood. 1976; 47:545–554. [PubMed: 1260119]

34. Barbieri SS, et al. Apocynin prevents cyclooxygenase 2 expression in human monocytes through NADPH oxidase and glutathione redox-dependent mechanisms. Free Radic Biol Med. 2004; 37:156–165. [PubMed: 15203187]

35. Francescone R, et al. Cytokines, IBD, and colitis-associated cancer. Inflamm Bowel Dis. 2015; 21:409–418. [PubMed: 25563695]

36. Sandborn WJ, et al. OCTAVE Induction 1, OCTAVE Induction 2, and OCTAVE Sustain Investigators. Tofacitinib as induction and maintenance therapy for ulcerative colitis. N Engl J Med. 2017; 376:1723–1736. [PubMed: 28467869]

37. Yokoyama S, et al. Tofacitinib, a janus kinase inhibitor demonstrates efficacy in an IL-15 transgenic mouse model that recapitulates pathologic manifestations of celiac disease. J Clin Immunol. 2013; 33:586–594. [PubMed: 23269601]

38. Traynor K. FDA approves tofacitinib for rheumatoid arthritis. Am J Health Syst Pharm. 2012; 69:2120.

39. Campregher C, et al. The position of the amino group on the benzene ring is critical for mesalamine's improvement of replication fidelity. Inflamm Bowel Dis. 2010; 16:576–582. [PubMed: 19821510]

40. Kortüm B, et al. Mesalazine and thymoquinone attenuate intestinal tumour development in Msh2(loxP/loxP) Villin-Cre mice. Gut. 2015; 64:1905–1912. [PubMed: 25429050]

41. Zienolddiny S, et al. Induction of microsatellite mutations by oxidative agents in human lung cancer cell lines. Carcinogenesis. 2000; 21:1521–1526. [PubMed: 10910953]

42. Turker MS, et al. A novel signature mutation for oxidative damage resembles a mutational pattern found commonly in human cancers. Cancer Res. 1999; 59:1837–1839. [PubMed: 10213488]

43. Gille JJ, et al. Mutagenicity of metabolic oxygen radicals in mammalian cell cultures. Carcinogenesis. 1994; 15:2695–2699. [PubMed: 8001223]

44. Moraes EC, et al. Mutagenesis by hydrogen peroxide treatment of mammalian cells: a molecular analysis. Carcinogenesis. 1990; 11:283–293. [PubMed: 2302755]

45. Akman SA, et al. *In vivo* mutagenesis of the reporter plasmid pSP189 induced by exposure of host Ad293 cells to activated polymorphonuclear leukocytes. Carcinogenesis. 1996; 17:2137–2141. [PubMed: 8895480]

46. Lee SY, et al. Microsatellite alterations at selected tetranucleotide repeats are associated with morphologies of colorectal neoplasias. Gastroenterology. 2010; 139:1519–1525. [PubMed: 20708618]

47. Tseng-Rogenski SS, et al. Oxidative stress induces nuclear-to-cytosol shift of hMSH3, a potential mechanism for EMAST in colorectal cancer cells. PLoS One. 2012; 7:e50616. [PubMed: 23226332]

48. Lee SY, et al. Microsatellite instability, EMAST, and morphology associations with T cell infiltration in colorectal neoplasia. Dig Dis Sci. 2012; 57:72–78. [PubMed: 21773681]

49. de Miranda NF, et al. Infiltration of Lynch colorectal cancers by activated immune cells associates with early staging of the primary tumor and absence of lymph node metastases. Clin Cancer Res. 2012; 18:1237–1245. [PubMed: 22261803]

50. Takemoto N, et al. The correlation of microsatellite instability and tumor-infiltrating lymphocytes in hereditary non-polyposis colorectal cancer (HNPCC) and sporadic colorectal cancers: the significance of different types of lymphocyte infiltration. Jpn J Clin Oncol. 2004; 34:90–98. [PubMed: 15067103]

51. Shacter E, et al. Activated neutrophils induce prolonged DNA damage in neighboring cells. Carcinogenesis. 1988; 9:2297–2304. [PubMed: 2847879]

52. Daig R, et al. Increased interleukin 8 expression in the colon mucosa of patients with inflammatory bowel disease. Gut. 1996; 38:216–222. [PubMed: 8801200]

53. Mitsuyama K, et al. Colonic mucosal interleukin-6 in inflammatory bowel disease. Digestion. 1991; 50:104–111. [PubMed: 1804734]

54. Braegger CP, et al. Tumour necrosis factor alpha in stool as a marker of intestinal inflammation. Lancet. 1992; 339:89–91. [PubMed: 1345871]

55. Couto D, et al. Scavenging of reactive oxygen and nitrogen species by the prodrug sulfasalazine and its metabolites 5-aminosalicylic acid and sulfapyridine. Redox Rep. 2010; 15:259–267. [PubMed: 21208525]

56. Miyachi Y, et al. Effect of sulphasalazine and its metabolites on the generation of reactive oxygen species. Gut. 1987; 28:190–195. [PubMed: 2881849]

57. Campregher C, et al. Mesalazine reduces mutations in transforming growth factor beta receptor II and activin type II receptor by improvement of replication fidelity in mononucleotide repeats. Clin Cancer Res. 2010; 16:1950–1956. [PubMed: 20197483]

58. Li Y, et al. Disease-related expression of the IL6/STAT3/SOCS3 signalling pathway in ulcerative colitis and ulcerative colitis-related carcinogenesis. Gut. 2010; 59:227–235. [PubMed: 19926618]

59. Li Y, et al. IL-6-induced DNMT1 activity mediates SOCS3 promoter hypermethylation in ulcerative colitis-related colorectal cancer. Carcinogenesis. 2012; 33:1889–1896. [PubMed: 22739025]
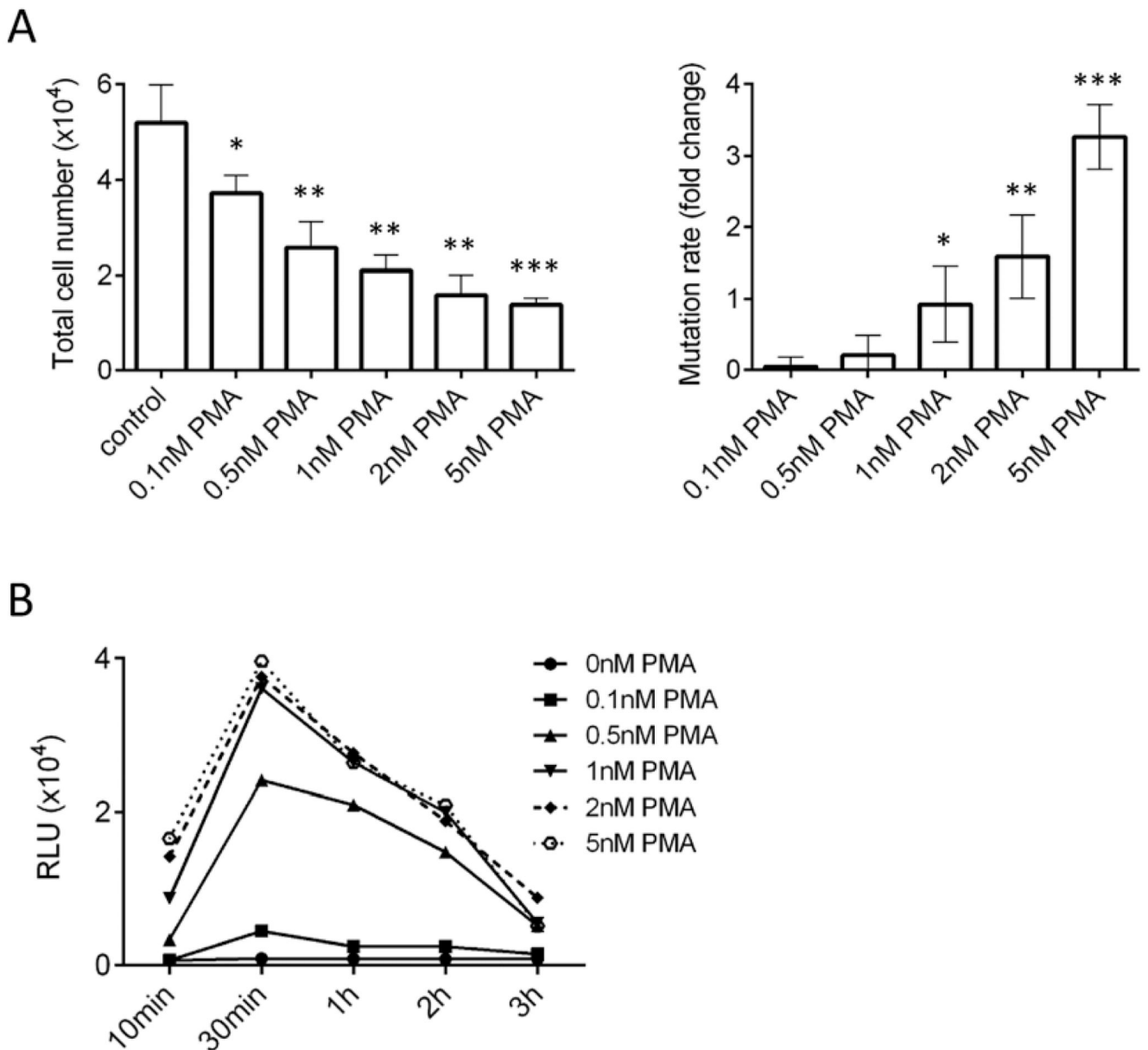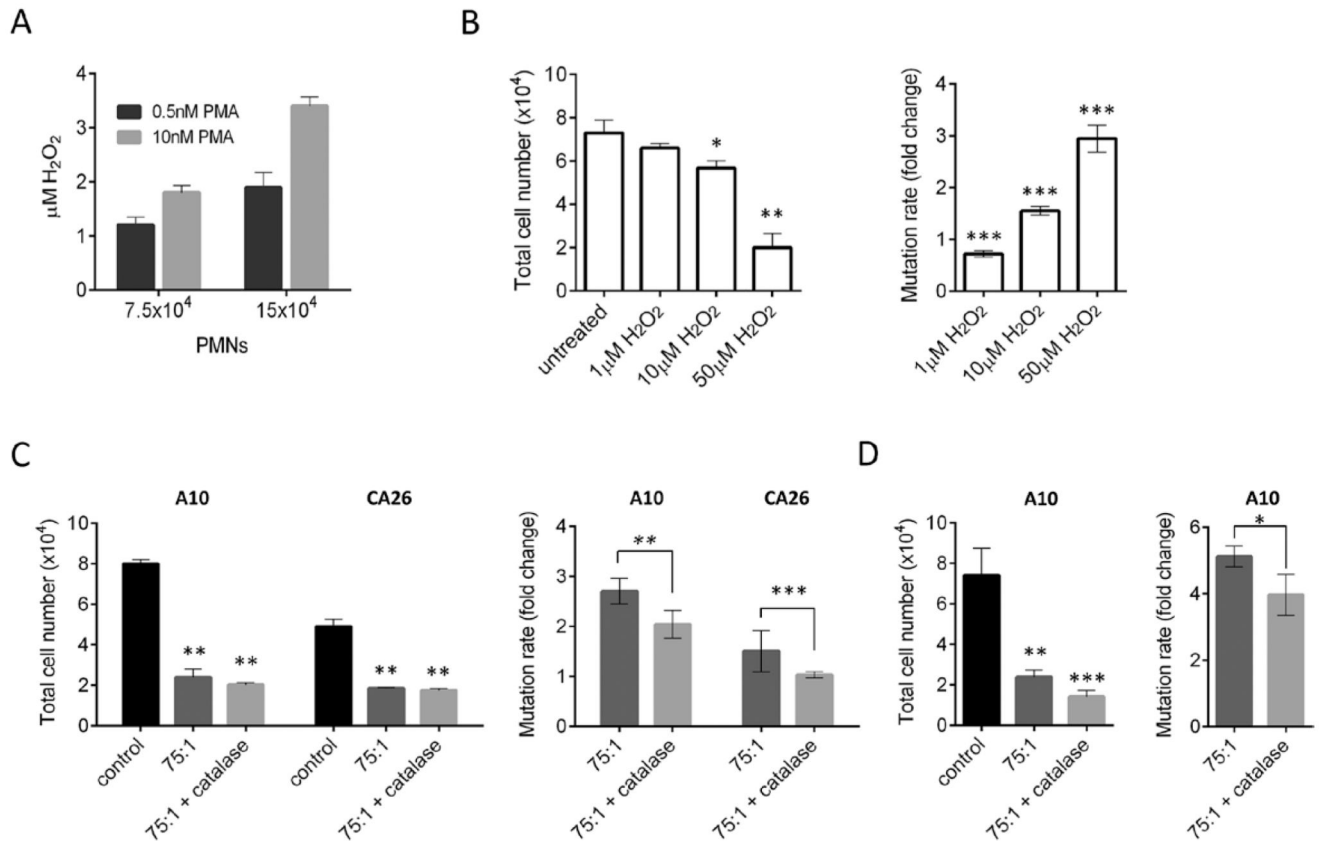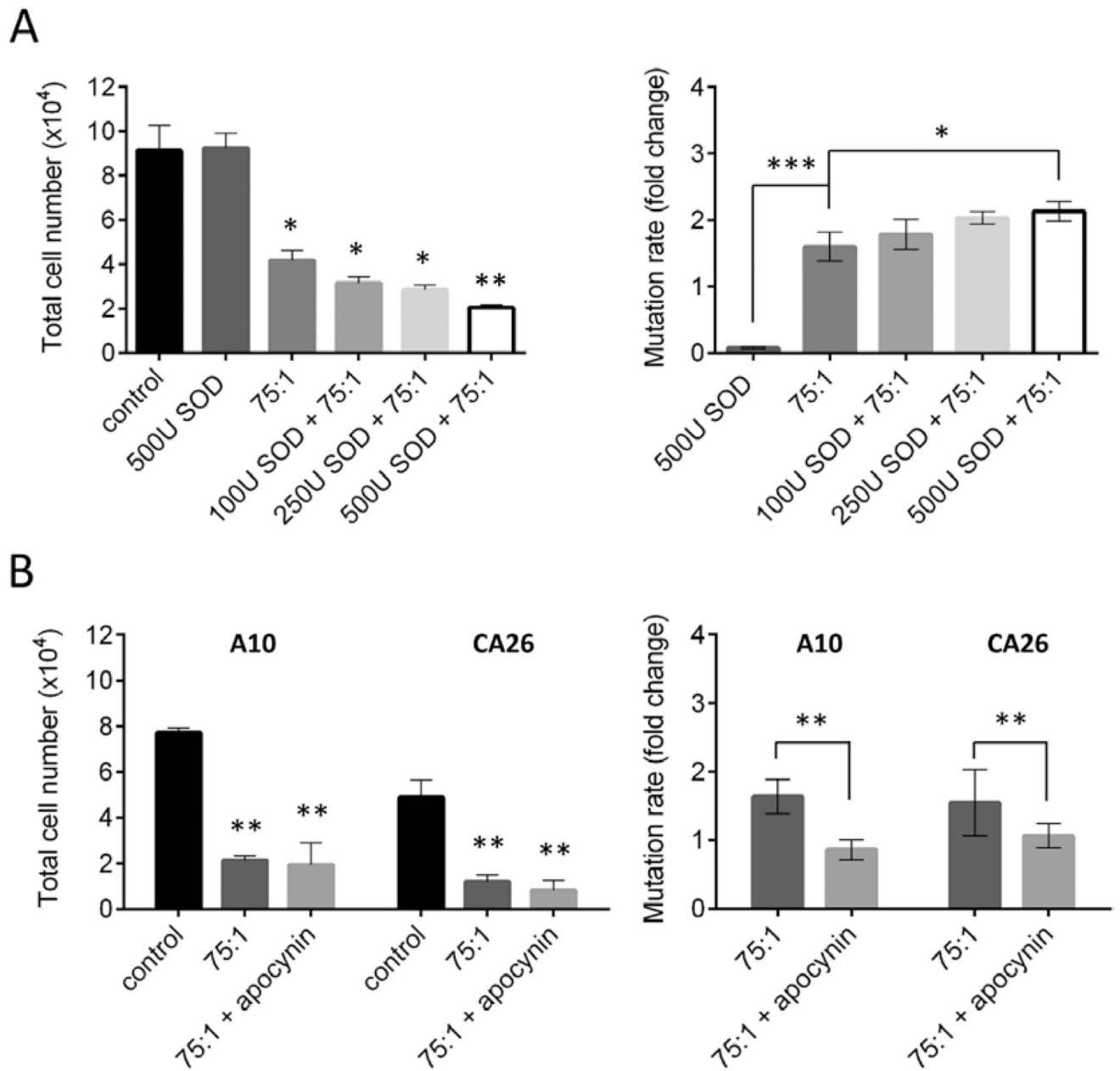
Figure 1.

Optimization of PMN activation by various PMA concentrations. (**A**) 5×10^3 EGPF-negative HCT116 + chr3-G16 cells were sorted by flow cytometry and treated with 0.1–5 nM PMA the following day for 24 h. PMA was removed and cells were grown until flow cytometric analysis on day 7. PMA dose dependently decreased cell count (left panel).The MR is presented as fold change to untreated control cells (right panel). PMA above 1 nM increased MR. All measurements were carried out in quadruplicates; *$P < 0.05$, **$P < 0.01$, ***$P < 0.001$. (**B**) A lucigenin-amplified chemiluminescence assay was used to determine superoxide release (expressed as relative light units [RLU]) upon activation of PMNs with PMA. After 30 min of activation, superoxide release was at its maximum. Single measurements were carried out.
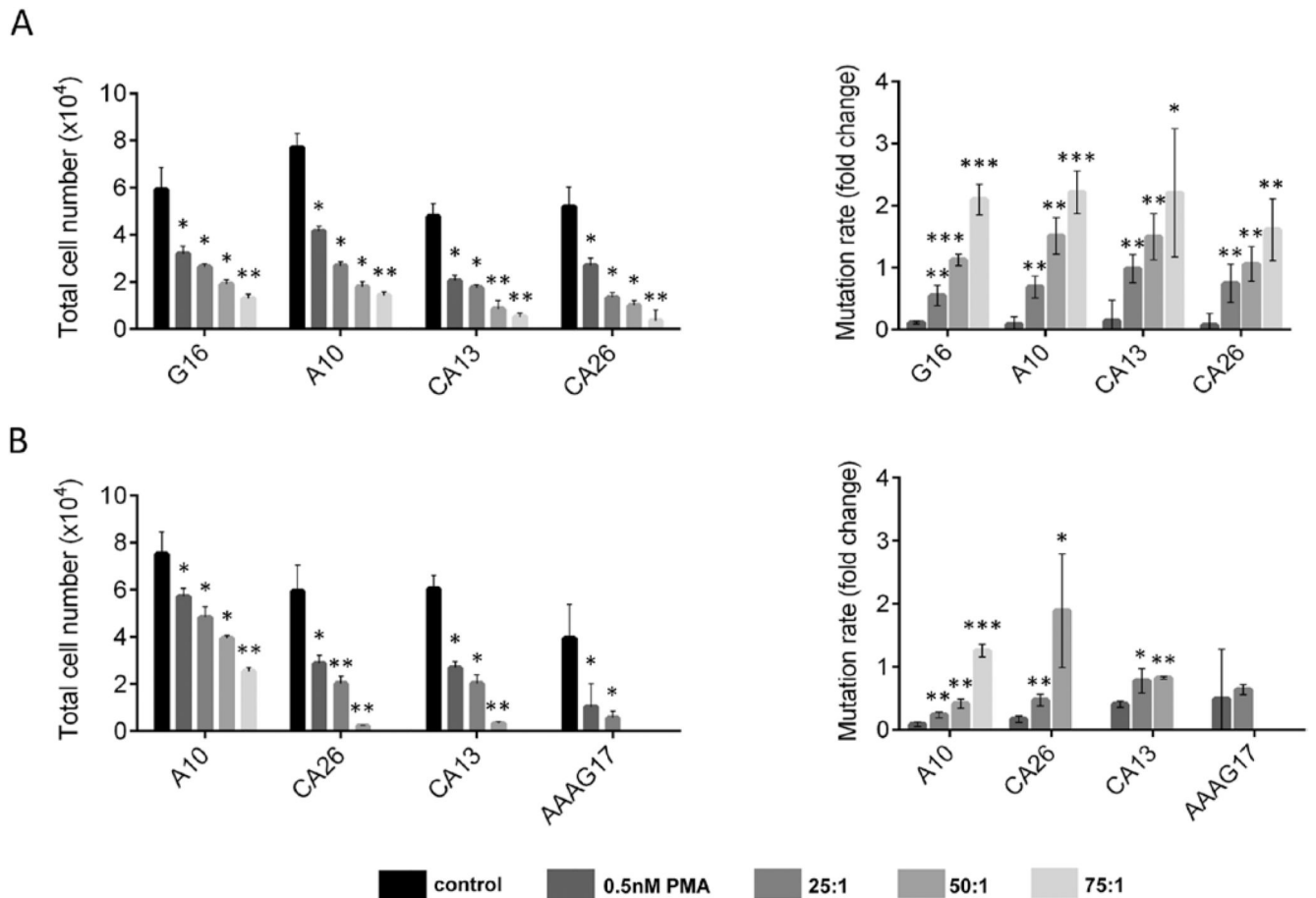
Figure 2.
Induction of frameshift mutations at mono-, di- and tetranucleotide repeats by co-culture of activated PMNs and HCT116 + chr3 (**A**) or HCEC-1CT (**B**). 5×10^3 EGPF-negative reporter cells were sorted on a FACSaria instrument and were incubated with PMA-activated (0.5 nM) PMNs at different effector (PMNs):target (epithelial cells) ratios the following day for 24 h. flow cytometric analysis was performed 6 days later showing a dose-dependent decrease in cell numbers and an increase in MR (presented as fold change to untreated control cells) for all clones. Measurements were carried out in quadruplicates. *$P < 0.05$, **$P < 0.01$,*** $P < 0.001$ compared with 0.5 nM PMA-treated control cells.

Figure 3.
Catalase reduces PMN-induced MSI. (**A**) H_2O_2 release from PMNs 30 min after PMA activation as measured by H_2O_2 Assay Kit (Abcam). (**B**) HCT116 + chr3-A10 cells were treated with H_2O_2 for 24 h. Flow cytometric analysis was performed 6 days later showing a dose-dependent decrease in cell numbers and an increase in MRs, which are presented as fold changes to untreated cells. (**C**) HCT116 + chr3-A10 and HCT116 + chr3-[CA]26 cell lines were co-cultured with activated PMNs at an effector:target ratio of 75:1. Catalase at 250 U/ml significantly reduced PMN-induced frameshift mutations without affecting cell growth. (**D**) Similarly, catalase also reduced mutations in HCEC-1CT-A10 cells. *$P < 0.05$, **$P < 0.01$.
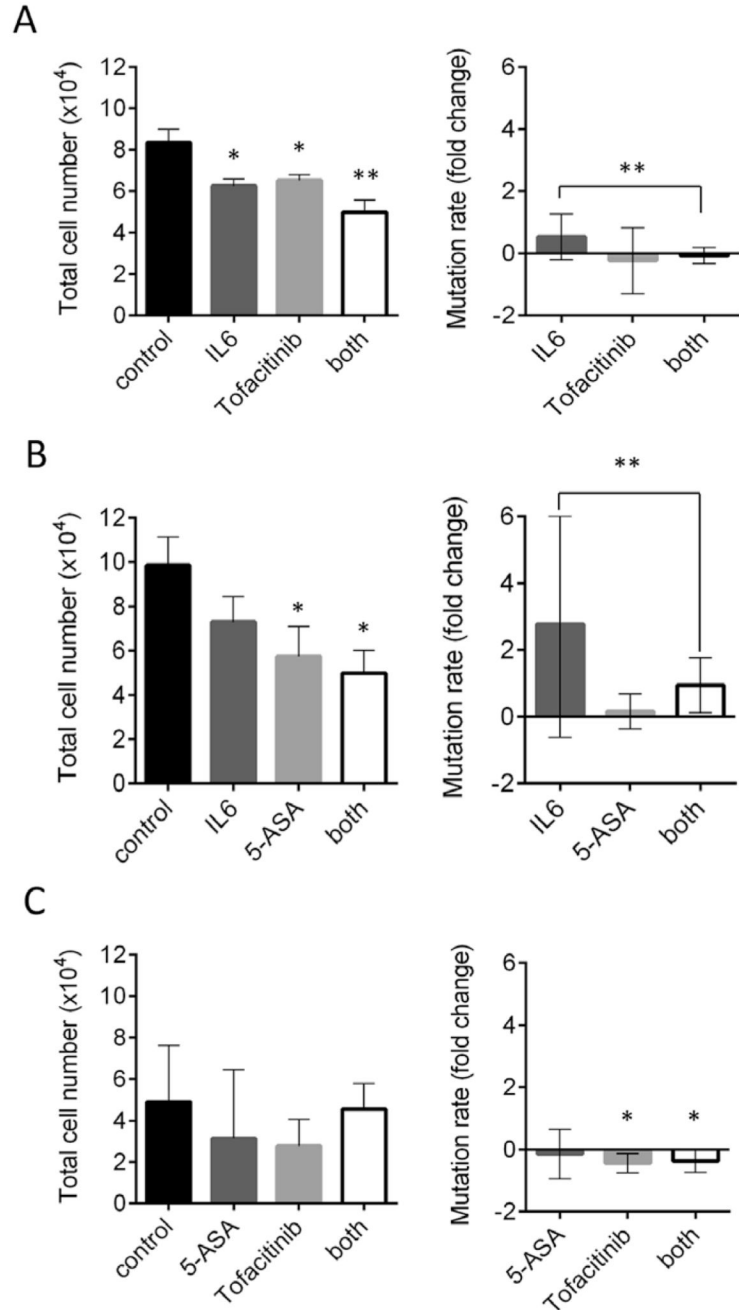
Figure 4.
Effect of SOD and apocynin on frameshift mutations. (**A**) SOD, catalyzing the dismutation of O_2^- into O_2 and H_2O_2, increased MR and decreased cell count in HCT16 + chr3-A10 in a dose-dependent manner. (**B**) The NADPH-oxidase inhibitor apocynin blocks the oxidative burst in PMNs. When used in co-culture, apocynin lowered PMN-induced frameshift mutations in both HCT116 + chr3-A10 and HCT116 + chr3-[CA]26 clones without affecting cell counts.
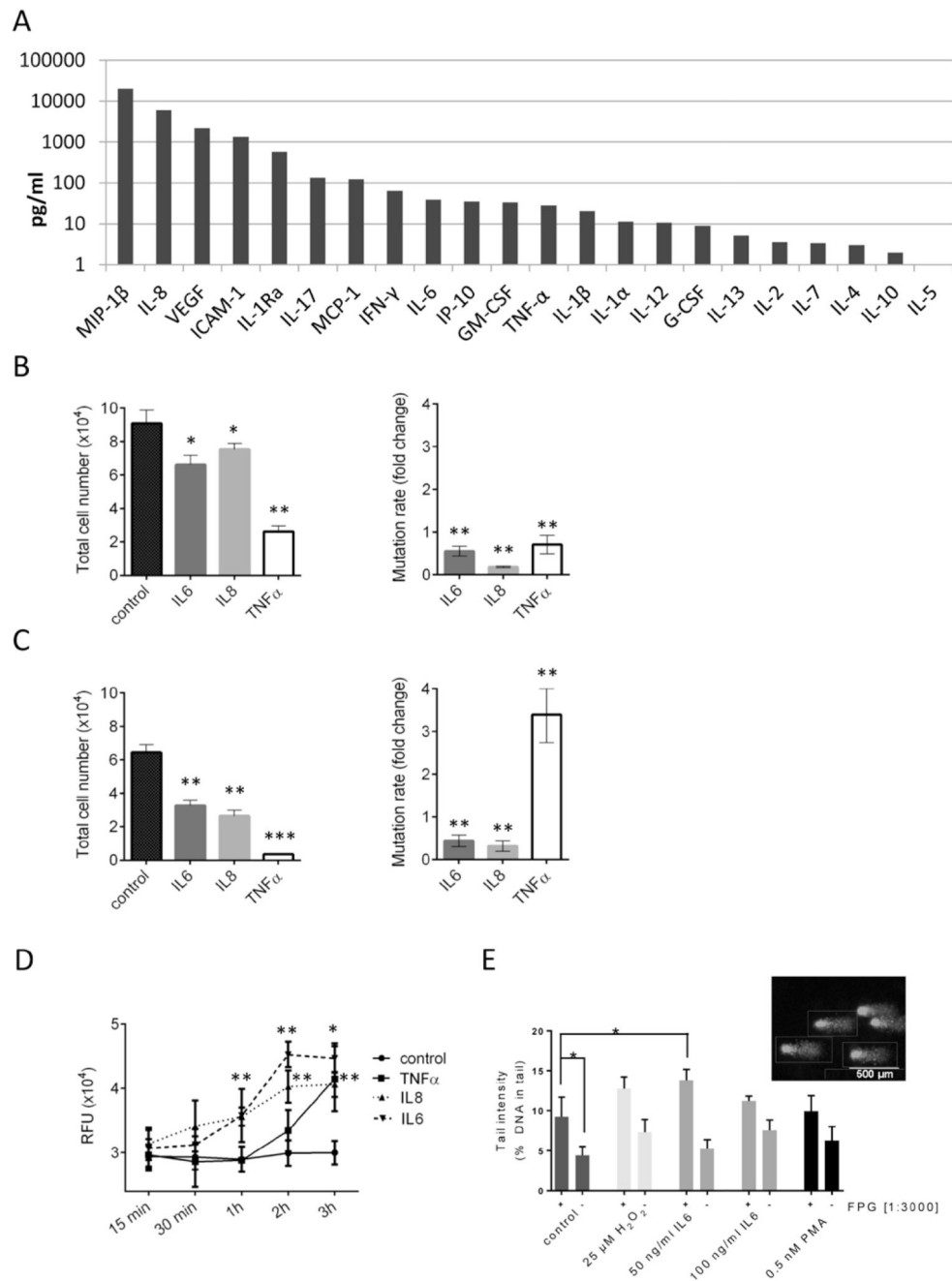
Figure 5.
PMN-released cytokines may induce frameshift mutations, internal ROS production and DNA oxidation. (**A**) 2×10^6 PMNs were activated with 0.5 nM PMA for 16 h and supernatants were subjected to a bead-based cytokine assay (Biorad) measured on a Bio-plex 200 instrument (Biorad). Treatment with 25 ng/ml IL-6, IL-8 or TNF-α decreased cell count and increased MR in HCT116 + chr3-A10 (**B**) or HCEC-1CT-[CA]26 (**C**). (**D**) Culture of HCEC-1CT with 25 ng/ml IL-6, IL-8 or TNF-α induced internal ROS production (as measured by DCFDA and expressed as relative fluorescent units, RFU) in a time-dependent

manner, with the highest upregulation at 3 h. (**E**) HCT116 + chr3 cells were exposed to IL-6, PMA or H_2O_2 for 24 h. The formation of oxidized purines (8-oxo-dG) was analyzed with and without FPG. DNA migration was evaluated using single cell gel electrophoresis and computer-aided analysis. Bars indicate means ± SD of results obtained from 150 cells from three slides each experimental condition (*t*-test).

Figure 6.
JAK inhibition and 5-ASA counteract the mutagenic effect of IL-6, but only JAK inhibition reduced PMN-induced MSI. (**A**) Treatment of HCT116 + chr3-[CA]26 with tofacitinib, a JAK inhibitor, neutralized IL-6-induced frameshift mutations. Total cell number decreased upon treatment with IL6 and/or tofacitinib. (**B**) Similarly, 5-ASA also reduced IL-6 induced frameshift mutations in HCT116 + chr3-[CA]26. 5-ASA decreased cell count, which was further diminished upon IL6 treatment. 5-ASA decreased cell number both of untreated and IL-6-treated cells. (**C**) 1×10^4 EGPF-negative HCT116 + chr3-[CA]26 were sorted in 24

wells. Twenty-four hours later, cells were treated with 5 mM 5-ASA and/or 2 μM tofacitinib before the addition of PMA-activated PMNs at an effector:target ratio of 75:1. Flow cytometric analysis was performed 7 days later. Tofacitinib counteracted PMN-induced frameshift mutations (which is presented as fold change to cells treated with PMA-activated PMNs only), whereas 5-ASA failed to do so. No additive effects were present.